

Technical Note

Dual-Frequency Microwave Plasma Source Based on Microwave Coaxial Transmission Line

Chi Chen , Wenjie Fu *, Chaoyang Zhang , Dun Lu , Meng Han  and Yang Yan

School of Electronic Science and Engineering, University of Electronic Science and Technology of China, Chengdu 610054, China; chenchi@std.uestc.edu.cn (C.C.); chaoyangzhang@std.uestc.edu.cn (C.Z.); ludun@std.uestc.edu.cn (D.L.); 201711040132@std.uestc.edu.cn (M.H.); yanyang@uestc.edu.cn (Y.Y.)

* Correspondence: fuwenjie@uestc.edu.cn

Featured Application: In various microwave plasma fields, such as Microwave Plasma Chemical Vapor Deposition (MPCVD), the dual-frequency plasma source could be used to control plasma characteristics flexibly.

Abstract: A dual-frequency plasma source has many advantages in applications. In this paper, a dual-frequency microwave plasma source is presented. This microwave plasma source is based on a coaxial transmission line without the resonator, and it can be operated in a wide band frequency region. Two microwaves are inputted from two ports into the plasma reactor: one is used firstly to excite the plasma and the other one is used to adjust plasma characteristics. Based on the COMSOL Multiphysics simulation, the experiment is carried out. In the experimental investigation, the plasma electron density and electron temperature can be controlled, respectively, by feeding in different frequencies from the second port, causing the particles at different energy levels to present different frequencies. This exploratory research improves the operation frequency of dual-frequency microwave plasma sources from RF to microwave.

Keywords: microwave plasma; dual-frequency plasma; electron temperature; electron density



Citation: Chen, C.; Fu, W.; Zhang, C.; Lu, D.; Han, M.; Yan, Y. Dual-Frequency Microwave Plasma Source Based on Microwave Coaxial Transmission Line. *Appl. Sci.* **2021**, *11*, 9873. <https://doi.org/10.3390/app11219873>

Academic Editor: Mariusz Jasiński

Received: 6 October 2021

Accepted: 19 October 2021

Published: 22 October 2021

Publisher's Note: MDPI stays neutral with regard to jurisdictional claims in published maps and institutional affiliations.



Copyright: © 2021 by the authors. Licensee MDPI, Basel, Switzerland. This article is an open access article distributed under the terms and conditions of the Creative Commons Attribution (CC BY) license (<https://creativecommons.org/licenses/by/4.0/>).

1. Introduction

To control plasma characteristics flexibly, the dual-frequency plasma source has been proposed and investigated [1–8]. The dual-frequency plasma source is a hybrid source, in which one frequency is chosen to be much higher than the other in order to achieve independent control of ion bombardment and electron density [9]. Research shows that, in plasma etching, dual-frequency operating could reduce particle contamination in the plasma reactor [10], and in the plasma-enhanced chemical vapor deposition (PECVD), dual-frequency operating could improve the film stress, step coverage, chemical composition, and film stability [11–14].

In previous studies, the exciting frequency for dual-frequency plasma sources mostly were mostly radio frequency (RF), such as 13.56 MHz, 27.12 MHz, 320 MHz, 340 kHz, and 40 kHz, and the structures of the plasma reactor are mostly capacitively coupled plasma (CCP) and/or inductively coupled plasma (ICP). In recent years, more and more microwave plasma sources have been proposed and applied [15–18]. However, dual-frequency microwave plasma sources are rarely investigated. For most microwave plasma sources, the microwave is propagated through a waveguide, and the plasma is excited in a resonator. Different from CCP and ICP reactor structures [19], the size of the microwave resonator is dependent on microwave frequency, and it is difficult to resonate two non-harmonic frequencies in one resonator.

Here, a microwave coaxial transmission line is introduced as the reactor for a dual-frequency microwave plasma source. In the coaxial transmission line, the electromagnetic wave mode of the microwave is TEM mode, and ultra-wide band electromagnetic waves,

from low-frequency wave to millimeter wave, could be inputted and propagated. The 2450 and 915 MHz microwaves, which are widely used in industry, are adopted in this investigation. There are two ports to input the microwaves. The 2450 MHz microwave is inputted from one port to excite plasma, and the 915 MHz microwave is inputted from another to adjust the plasma characteristics. To investigate the characteristics of dual-frequency microwave plasma, the microwave is inputted from two ports to excite the plasma, and a comparison is conducted between single-frequency microwave plasma and dual-frequency microwave plasma in the same reactor.

2. Experiment Design

The schematic diagram for the presented dual-frequency microwave plasma source based on the microwave coaxial transmission line is shown in Figure 1.

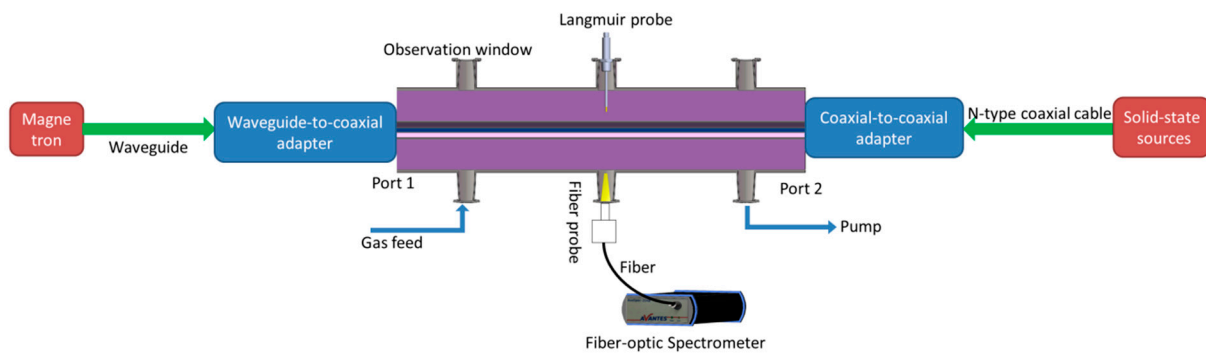


Figure 1. Schematic of the coaxial line plasma driven by the dual microwave sources.

The plasma reactor is a coaxial line, whose outer diameter is 150 mm and the inner diameter is 8 mm. A quartz glass tube surrounds the inner conductor. Between the outer conductor and the quartz glass tube, there is a vacuum region in which the plasma is excited. There are two microwave ports at the two ends of the coaxial transmission line. One is used to input the 2450 MHz microwave, and another is used to input the 915 MHz microwave. A magnetron microwave power generator (ASTeX AX2110) is used to generate the continuous-wave 2450 MHz microwave. An isolation circulator with a water load in an isolated way is connected to the magnetron microwave power generator. In this way, the microwave feedback will be entirely absorbed by the water load. An ASTeX SmartMatch is used to match the impedance so that the maximum amount of power can be coupled with the plasma. The 2450 MHz microwave is transmitted from the generator to the plasma reactor by the waveguide. A waveguide-to-coaxial adapter is designed and installed to guide the microwave from the waveguide into the coaxial transmission line plasma reactor through Port 1 [15]. A custom-made solid-state microwave power source (Wattsine Electronic Technology Co., Ltd. Chengdu China) is used to generate a continuous-wave 915 MHz microwave. The 915 MHz microwave is transmitted by N-type coaxial cables. The incident and reflected powers are monitored by a bi-directional coaxial coupler and Keysight power meter (Narda N1914A). A coaxial-to-coaxial adapter is designed and installed to guide the microwave from the N-type coaxial cable into the coaxial transmission line plasma reactor through Port 2. A coaxial low-pass filter is installed into N-type coaxial cables to avoid the solid-state microwave power source affected by 2450 MHz.

There are several KF flanges on the outer conductor, which are used to connect a vacuum pump, gas feed mass flow meter, and diagnostic devices. A Langmuir probe and an optical emission spectrometry (OES) are used to diagnose and investigate the plasma characteristics from two KF flanges in the center of the plasma reactor.

The experimental processes are as follows: First, pump the pressure in the reactor below 10 Pa by a vacuum pump; second, adjust the argon flow rate at 15~20 sccm to stabilize the discharge pressure at 80 Pa by the mass flow meter; then, turn on the microwave source

at Port 1 to excite plasma discharge; finally, turn on the microwave source at Port 2 to adjust plasma characteristics and measure the plasma parameters.

As shown in Figure 1, the coaxial transmission line is a non-resonant structure. Thus, ultra-wide band electromagnetic waves could be inputted into the reactor. However, it would only be discharged at the area near the input Port 1, and not at the whole reactor. To produce a dual-frequency operation, the plasma must be affected by microwaves from both ports. Therefore, the plasma excited by 2450 MHz from Port 1 should be distributed in the whole reactor. To obtain the plasma distribution in the reactor, COMSOL Multiphysics is used to simulate the plasma distribution at different microwave powers from Port 1.

In this investigation, the argon plasma considered in the simulated model contains only electrons (e), positively charged argon ions (Ar^+), metastable-state argon (Ars), and argon (Ar) atoms. For these species, the main transportation equations are provided in Table 1 [20].

Table 1. Important collision processes in the argon discharge.

No.	Reaction	Type	Energy Loss $\Delta\epsilon$ (eV)
1	$e + Ar = e + Ar$	Elastic	
2	$e + Ar = e + Ars$	Excitation	11.5
3	$e + Ars = e + Ar$	Superelastic	-11.5
4	$e + Ars = 2e + Ar^+$	Ionization	15.8
5	$e + Ar = 2e + Ar^+$	Ionization	4.24
6	$Ars + Ars = e + Ar + Ar^+$	Penning ionization	
7	$Ars + Ar = Ar + Ar$	Metastable quenching	

Stepwise ionization (Reaction 5 in Table 1) plays an important role in sustaining low-pressure argon discharges. Excited argon atoms are consumed via superelastic collisions with electrons, quenching with neutral argon atoms, ionization, or Penning ionization where two metastable argon atoms react to form a neutral argon atom, an argon ion, and an electron. Reaction 7 is responsible for the heating of the gas. The 11.5 eV of energy, which was consumed in creating the electronically excited argon atom, returns to the gas as thermal energy when the excited metastable-state argon atoms quenching.

In the simulation, the electron energy distribution function (EEDF) is approximately set as the Maxwellian distribution function, due to the fact that the discharge pressure 80 Pa is greater than 6.66 Pa [21,22]. Although publications show that the plasma densities in simulations as Maxwellian distribution are higher than experimental measurements, they also show that the plasma distributions in simulations present good agreement with experimental measurements [23–26]. Therefore, the Maxwellian distribution function is still useful, and the plasma distributions at different exciting powers are normalized, presented in Figure 2.

As shown in Figure 2, the plasma discharge area is spread with increasing Port 1 microwave power. When the inputted 2450 MHz microwave power is at 500 W, the electron density near Port 2 is much lower than that near Port 1. When the inputted 2450 MHz microwave power is at 600 W, the electron density near Port 2 is a little lower than that near Port 1, but the plasma distribution is still non-uniform. When the inputted 2450 MHz microwave power is at 700 W, the electron density near Port 1 is nearly the same as that near Port 2, and in the area between Port 1 and Port 2, the plasma distribution is approximately uniform. While electron density is sufficiently affected by microwave power, the electron temperature is almost unaffected by microwave power changes. Therefore, the microwave power at Port 1 was set at 700 W to excite the plasma.

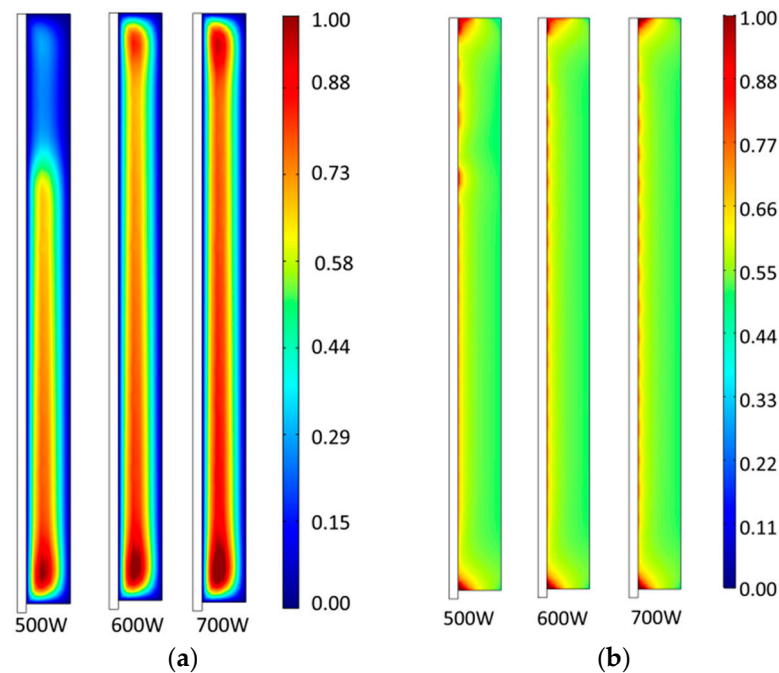


Figure 2. COMSOL simulation of the electron density and temperature distributions at a fixed pressure of 80 Pa under Port 1 2450 MHz microwave power: (a) electron density (b) electron temperature.

3. Experiment Results

Based on the simulation results, the experiment was carried out in accordance with processes listed in Section 2. Firstly, the 700 W 2450 MHz microwave was inputted into the reactor from Port 1 at a pressure of 80 Pa. The plasma can be excited with the assistance of an automatic impedance matchbox. In the center of the plasma reactor, the electron density and temperature measured by the Langmuir probe were $n_e = 1.56 \times 10^{16} \text{ m}^{-3}$ and $T_e = 2.46 \text{ (eV)}$.

For microwave-excited plasma, electrons oscillate among the heavy immobile ions at the plasma electron frequency. At this time, if another microwave with the frequency below the plasma electron frequency is inputted from another port, the inertia of the electrons is sufficiently low for them to respond to the electric field in the incident electromagnetic wave, and the electron can, therefore, absorb energy from it. If the frequency of the incident microwave is higher than the electron plasma frequency, the inertia of an electron would be too high to enable it to respond fully to the incident microwave. Therefore, the interaction of the microwave with individual electrons is relatively insignificant. Thus, different interaction modes of microwaves with electrons can be achieved by controlling the frequencies of the second incident microwaves [27].

The electron plasma frequency is a function of the electron number density and is given by [27].

$$\omega_{pe} = 2\pi\nu_{pe} = \sqrt{\frac{n_e e^2}{\epsilon_0 m_e}} \quad (\text{rad/s}) \quad (1)$$

where ν_{pe} is the electron number density in Hz. The n_e is the electron density, the ϵ_0 is the permittivity of free space, and the m_e is the mass of an electron. According to Equation (1), for $n_e = 1.56 \times 10^{16} \text{ m}^{-3}$, the electron plasma frequency is $\nu_e = 1123 \text{ MHz}$, which is located between 2450 MHz and 915 MHz. Then, if the input microwave from Port 2 is 2450 or 915 MHz, the plasma would show different responding behaviors.

To compare with the influence of the 915 MHz microwave, a 2450 MHz solid-state source was used instead of the 915 MHz solid-state source and the low-pass filter for comparative experiments. In the experiment, 915 and 2450 MHz microwaves were inputted from Port 2 to investigate the plasma characteristics changes, respectively. Figure 3

shows the effect of microwave inputted from Port 2 on the electron density and electron temperature measured by the Langmuir probe.

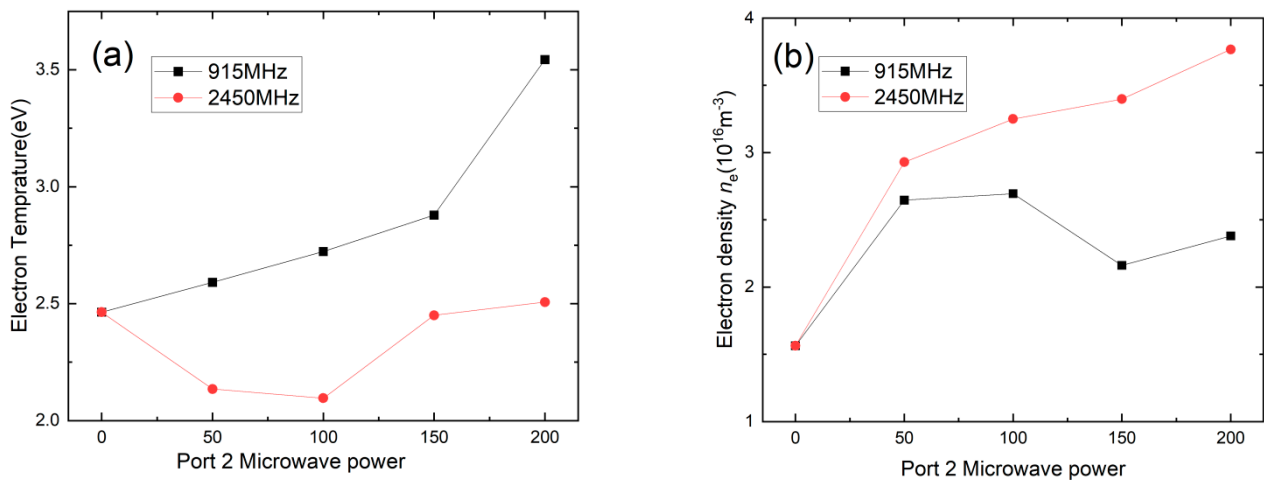


Figure 3. Effect of the microwave inputted from port 2 measured by the Langmuir probe: (a) electron temperature; (b) electron density.

Figure 3a shows that, when the second microwave was inputted from Port 2, the plasma electron temperature gradually increased as the 915 MHz microwave power increased and did not change sufficiently as the 2450 MHz microwave power increased. In contrast, Figure 3b shows that, when the second microwave was inputted from Port 2, the plasma electron density did not change sufficiently as the 915 MHz microwave power increased, but it gradually increased as the 2450 MHz microwave power increased.

This means that the second incident microwaves with frequencies below the plasma electron frequency could increase the electron temperature and affect the electron density indistinctly, and the second incident microwaves with frequencies above the plasma electron frequency could increase the electron density and affect the electron temperature indistinctly.

To investigate the physical mechanism of these phenomena, the OES results at different conditions were analyzed, and the OES data were all obtained at 10-ms integral times. The spectrum at only 700 W 2450 MHz microwave that was inputted from Port 1 acquired by the OES method is presented in Figure 4.

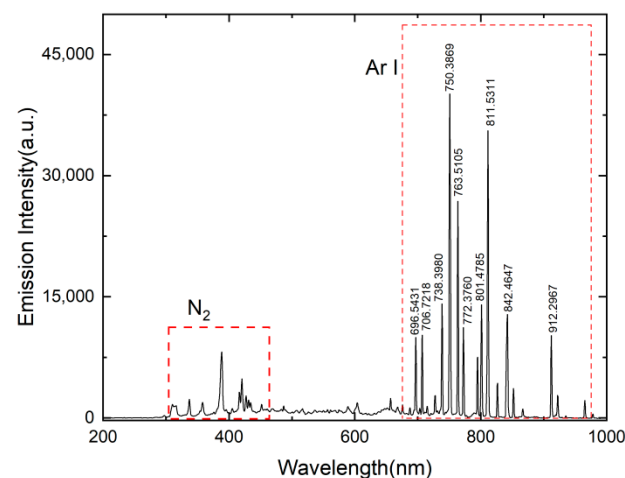


Figure 4. Spectrum of the coaxial line plasma driven by the 2450 MHz microwave from Port 1 at a power of 700 W and pressure of 80 Pa.

The spectrum result presents two main particles in plasma: nitrogen molecule (N_2) and Ar. The N_2 comes from air residue. In the experiment, the intensity of the Ar I line group was much higher than the others. In the Ar I line group, the characteristic peaks at Ar I 750.3869 nm, and Ar I 811.5311 nm were quite obvious with the highest intensity.

The OES data at the 200 W–915 MHz microwave that was inputted from Port 2 and at the 200 W–2450 MHz microwave that was inputted from Port 2 are presented in Figure 5a,b, respectively.

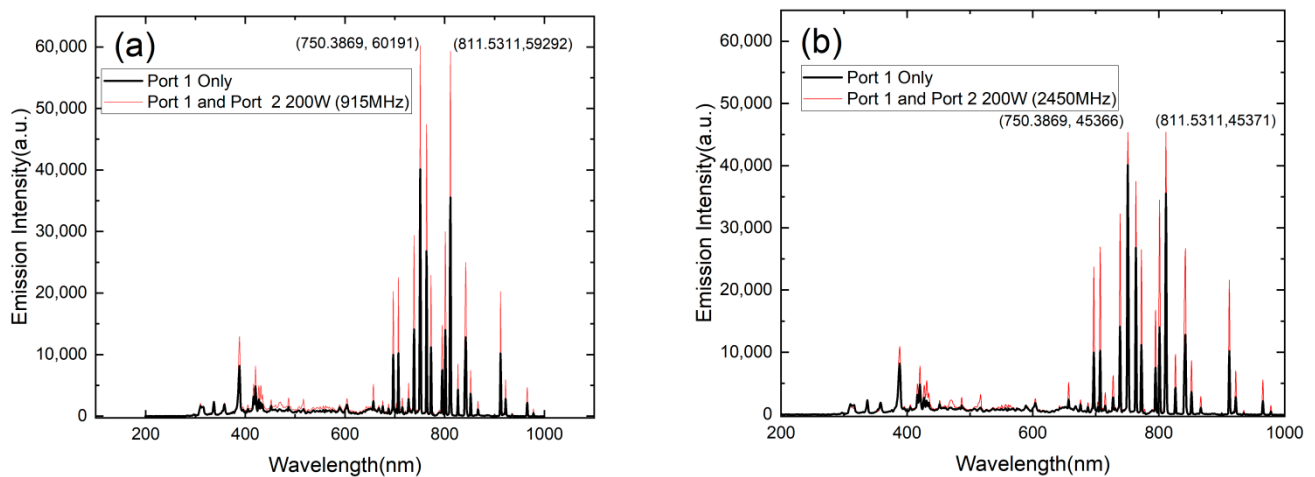


Figure 5. Spectrum of microwave inputted from Port 2 at the power of 200 W: (a) 915 MHz microwave; (b) 2450 MHz microwave.

In Figure 5, it is obviously seen that the intensity of the Ar I characteristic peaks was sufficiently improved when both 915 and 2450 MHz microwaves were inputted, and different Ar I characteristic peaks show different changes. The intensity of the two highest Ar I characteristic peaks (750.3869 and 811.5311 nm) at the 915 MHz microwave that was inputted from Port 2 were higher than that of the 2450 MHz microwave that was inputted from Port 2. Meanwhile, the intensity of other Ar I characteristic peaks (such as 696.5431 nm, 706.7218 nm, 772.3760 nm) at the 915 MHz microwave that was inputted from Port 2 are lower than that of the 2450 MHz microwave that was inputted from Port 2.

The intensity changes of several Ar I characteristic peaks versus microwave power that were inputted from Port 2 are shown in Figure 6.

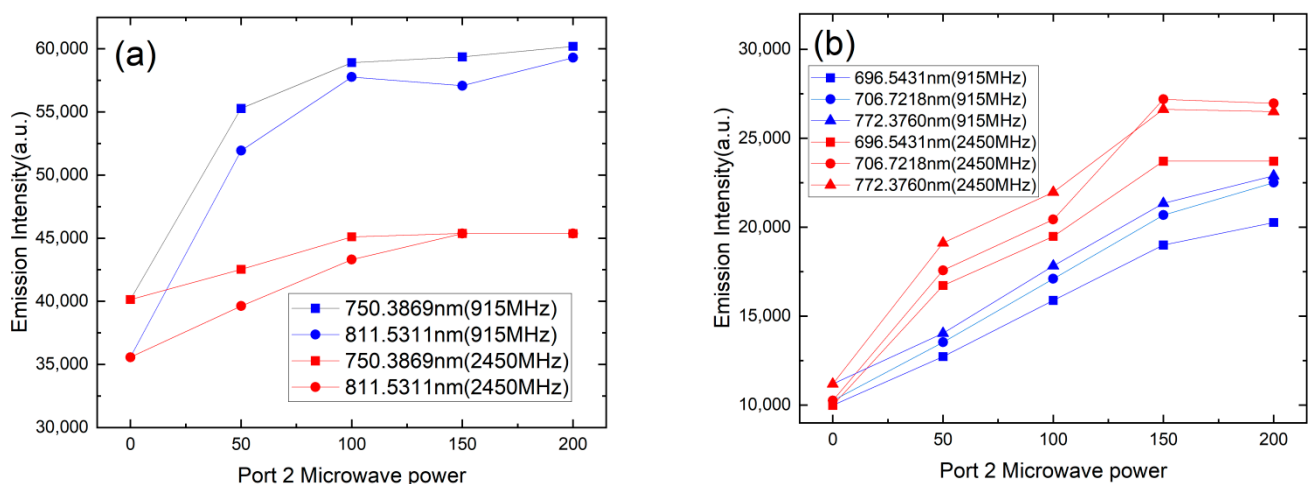


Figure 6. Intensity changes of Ar I characteristic peaks versus microwave power inputted from port 2 (a) 750.3869 and 811.5311 nm; (b) 696.5431, 706.7218 and 772.3760 nm.

The OES results show that when the intensity of the characteristic peaks is higher at only 700 W 2450 MHz that was inputted from Port 1, the intensity increase is higher at 915 MHz that was inputted from Port 2 than at 2450 MHz that was inputted from Port 2 (Table S1, Figure S1). This indicates that particles at different energy levels presented different responses to different frequencies. In addition, the particles at different energy levels contributed different ratios in plasma electron density and electron temperature, thus, different frequencies could selectively control the plasma characteristics.

4. Summary and Discussion

Based on the COMSOL Multiphysics simulation, a dual-frequency microwave plasma source is proposed and investigated. This dual-frequency microwave plasma source is based on the coaxial transmission line, and 2450 and 915 MHz microwaves are utilized in this study.

In the experiment, the plasma was excited by a 2450 MHz microwave from Port 1 first, and then a 915 MHz microwave was inputted from Port 2 to adjust the plasma characteristics. The measured experiment results by the Langmuir probe show that the electron temperature gradually increases as the 915 MHz microwave power increases, and there is little change in electron density. In contrast, if there is a 2450 MHz microwave that is inputted from Port 2, the electron density increases as the microwave power increases, and there is little change in the electron temperature. These phenomena of dual-frequency microwave plasma are similar to dual-frequency RF plasma.

The OES method is used to investigate the physical mechanism of these phenomena, and the OES results show that the particles at different energy levels presented different responses to different frequencies. Thus, different frequencies could selectively control the plasma characteristics. If a high-power wide bandwidth frequency tunable microwave source is used as the power source from Port 2, the plasma electron density and electron temperature would be controlled, respectively and precisely, in the dual-frequency microwave plasma source. This exploratory research would improve the operation frequency of dual-frequency microwave plasma sources from RF to microwave.

Supplementary Materials: The following are available online at <https://www.mdpi.com/article/10.3390/app11219873/s1>, Table S1: Intensity of Ar I characteristic peaks, Figure S1: Intensity of Ar I characteristic peaks versus microwave power inputted from port 2 under pressure of 80 Pa and 700 W 2450 MHz microwave at Port 1.

Author Contributions: C.C. and W.F. contributed to the overall study design, analysis, and writing of the manuscript. C.Z., D.L., M.H. and Y.Y. provided technical support and revised the manuscript. All authors have read and agreed to the published version of the manuscript.

Funding: This work was supported by the National Key Research and Development Program of China under 2019YFA0210202, the National Natural Science Foundation of China under Grant 61971097 and 62111530054.

Conflicts of Interest: The authors declare no conflict of interest.

References

1. Shin, K.S.; Sahu, B.B.; Han, J.G.; Hori, M. Utility of dual frequency hybrid source for plasma and radical generation in plasma enhanced chemical vapor deposition process. *Jpn. J. Appl. Phys.* **2015**, *54*, 76201. [CrossRef]
2. van de Ven, E.P.; Connick, I.W.; Harrus, A.S. Advantages of dual frequency PECVD for deposition of ILD and passivation films. In Proceedings of the Seventh International IEEE Conference on VLSI Multilevel Interconnection, Santa Clara, CA, USA, 12–13 June 1990.
3. Lafleur, T.; Delattre, P.A.; Johnson, E.V.; Booth, J.P. Separate control of the ion flux and ion energy in capacitively coupled radio-frequency discharges using voltage waveform tailoring. *Appl. Phys. Lett.* **2012**, *101*, 124104. [CrossRef]
4. Curley, G.A.; Marić, D.; Booth, J.; Corr, C.S.; Chabert, P.; Guillon, J. Negative ions in single and dual frequency capacitively coupled fluorocarbon plasmas. *Plasma Sources Sci. Technol.* **2007**, *16*, S87–S93. [CrossRef]
5. Lee, J.K.; Manuilenko, O.V.; Babaeva, N.Y.; Kim, H.C.; Shon, J.W. Ion energy distribution control in single and dual frequency capacitive plasma sources. *Plasma Sources Sci. Technol.* **2005**, *14*, 89–97. [CrossRef]

6. Booth, J.P.; Curley, G.; Marić, D.; Chabert, P. Dual-frequency capacitive radiofrequency discharges: Effect of low-frequency power on electron density and ion flux. *Plasma Sources Sci. Technol.* **2010**, *19*, 15005. [[CrossRef](#)]
7. Schulze, J.; Schüngel, E.; Czarnetzki, U.; Donkó, Z. Optimization of the electrical asymmetry effect in dual-frequency capacitively coupled radio frequency discharges: Experiment, simulation, and model. *J. Appl. Phys.* **2009**, *106*, 63307. [[CrossRef](#)]
8. Maeshige, K.; Washio, G.; Yagisawa, T.; Makabe, T. Functional design of a pulsed two-frequency capacitively coupled plasma in CF₄/Ar for SiO₂ etching. *J. Appl. Phys.* **2002**, *91*, 9494. [[CrossRef](#)]
9. Pierrat, F.; Vallée, C.; Gassilloud, R.; Michallon, P.; Pelissier, B.; Caubet, P. PECVD RF versus dual frequency: An investigation of plasma influence on metal–organic precursors’ decomposition and material characteristics. *J. Phys. D Appl. Phys.* **2014**, *47*, 185201. [[CrossRef](#)]
10. Kim, M.; Cheong, H.; Whang, K. Particle formation and its control in dual frequency plasma etching reactors. *J. Vac. Sci. Technol. A Vac. Surf. Film.* **2015**, *33*, 41303. [[CrossRef](#)]
11. Cianci, E.; Schina, A.; Minotti, A.; Quaresima, S.; Foglietti, V. Dual frequency PECVD silicon nitride for fabrication of CMUTs’ membranes. *Sens. Actuators A Phys.* **2006**, *127*, 80–87. [[CrossRef](#)]
12. Pearce, C.W.; Fetcho, R.F.; Gross, M.D.; Koefer, R.F.; Pudliner, R.A. Characteristics of silicon nitride deposited by plasma-enhanced chemical vapor deposition using a dual frequency radio-frequency source. *J. Appl. Phys.* **1992**, *71*, 1838. [[CrossRef](#)]
13. Tarraf, A.; Daleiden, J.; Irmer, S.; Prasai, D.; Hillmer, H. Stress investigation of PECVD dielectric layers for advanced optical MEMS. *J. Micromechanics Microeng.* **2003**, *14*, 317–323. [[CrossRef](#)]
14. Zhou, X.; Tan, X.; Lv, Y.; Wang, Y.; Li, J.; Liang, S.; Zhang, Z.; Feng, Z.; Cai, S. 128-pixel arrays of 4H-SiC UV APD with dual-frequency PECVD SiNx passivation. *Opt. Express* **2020**, *28*, 29245. [[CrossRef](#)] [[PubMed](#)]
15. Chen, C.; Fu, W.; Zhang, C.; Lu, D.; Han, M.; Yan, Y. Langmuir Probe Diagnostics with Optical Emission Spectrometry (OES) for Coaxial Line Microwave Plasma. *Appl. Sci.* **2020**, *10*, 8117. [[CrossRef](#)]
16. Cha, J.; Kim, S.; Lee, H. A Linear Microwave Plasma Source Using a Circular Waveguide Filled with a Relatively High-Permittivity Dielectric: Comparison with a Conventional Quasi-Coaxial Line Waveguide. *Appl. Sci.* **2021**, *11*, 5358. [[CrossRef](#)]
17. Salgado-Meza, M.; Martínez-Rodríguez, G.; Tirado-Cantú, P.; Montijo-Valenzuela, E.E.; García-Gutiérrez, R. Synthesis and Properties of Electrically Conductive/Nitrogen Grain Boundaries Incorporated Ultrananocrystalline Diamond (N-UNCD) Thin Films Grown by Microwave Plasma Chemical Vapor Deposition (MPCVD). *Appl. Sci.* **2021**, *11*, 8443. [[CrossRef](#)]
18. Wiktor, A.; Hrycak, B.; Jasiński, M.; Rybak, K.; Kieliszek, M.; Kraśniewska, K.; Witrowa-Rajchert, D. Impact of Atmospheric Pressure Microwave Plasma Treatment on Quality of Selected Spices. *Appl. Sci.* **2020**, *10*, 6815. [[CrossRef](#)]
19. Zhang, Y.; Kushner, M.J.; Sriraman, S.; Marakhtanov, A.; Holland, J.; Paterson, A. Control of ion energy and angular distributions in dual-frequency capacitively coupled plasmas through power ratios and phase: Consequences on etch profiles. *J. Vac. Sci. Technol. A* **2015**, *33*, 31302. [[CrossRef](#)]
20. Kim, D.; Jeong, Y.; Shon, Y.; Kwon, D.; Jeon, J.; Choe, H. Modified Fluid Simulation of an Inductively Coupled Plasma Discharge. *Appl. Sci. Conver. Technol.* **2019**, *28*, 221–225. [[CrossRef](#)]
21. Franz, G. *Low Pressure Plasmas and Microstructuring Technology*; Springer: Berlin/Heidelberg, Germany, 2009; pp. 188–190.
22. Rebiai, S.; Bahouh, H.; Sahli, S. 2-D simulation of dual frequency capacitively coupled helium plasma, using COMSOL multi-physics. *IEEE Trans. Dielectr. Electr. Insul.* **2013**, *20*, 1616–1624. [[CrossRef](#)]
23. Ochoa Brezmes, A.; Breitkopf, C. Simulation of inductively coupled plasma with applied bias voltage using COMSOL. *Vacuum* **2014**, *109*, 52–60. [[CrossRef](#)]
24. Lei, F.; Li, X.; Liu, Y.; Liu, D.; Yang, M.; Yu, Y. Simulation of a large size inductively coupled plasma generator and comparison with experimental data. *AIP Adv.* **2018**, *8*, 15003.
25. Lymberopoulos, D.P.; Economou, D.J. Modeling and simulation of glow discharge plasma reactors. *J. Vac. Sci. Technol. A Vac. Surf. Film.* **1994**, *12*, 1229–1236. [[CrossRef](#)]
26. Shahbazian, A.; Salem, M.K.; Ghoranneviss, M. Simulation by COMSOL of Effects of Probe on Inductively Coupled Argon Plasma. *Braz. J. Phys.* **2021**, *51*, 351. [[CrossRef](#)]
27. Reece Roth, J. Principles. In *Industrial Plasma Engineering*; CRC Press: Boca Raton, FL, USA, 1995; Volume 1.